

THE ION-HOSE INSTABILITY IN HIGH-CURRENT MULTI-PULSE INDUCTION LINACS*

C. A. Ekdahl†, Los Alamos National Laboratory, Los Alamos, NM, USA

Abstract

The ion-hose instability has usually been considered a danger for long-pulse, high-current electron linear induction accelerators (LIAs). However, it is also a concern for multi-pulse LIAs. We have simulated this instability for the new Scorpius multi-pulse LIA. The simulations have shown that the magnetic focusing field designed for Scorpius will be strong enough to suppress ion-hose instability if the residual gas pressure is below a value that is readily attainable with the present designs of induction cells and other accelerator components.

INTRODUCTION

The ion hose instability [1] is a consequence of beam-electron ionization of residual gas in the accelerator. The space-charge of the high-energy beam ejects low-energy electrons from the ionized channel, leaving a positively-charged ion channel that attracts the electron beam. The beam can oscillate in the potential well around the channel position.

Likewise, the electron beam attracts the ions, which can oscillate about the beam position. Because of the vast differences in particle mass, the electron and ion oscillations are out of phase, and the oscillation amplitudes grow exponentially. The number of amplitude e-foldings is proportional to the channel ion density n_i [1, 2], which in turn is proportional to the residual gas pressure and electron beam pulse length. This scaling of the instability growth was demonstrated in experiments on the long-pulse DARHT-II accelerator at Los Alamos [3]. (DARHT is an acronym for Dual Axis Radiography for Hydrodynamic Tests.)

Although the ion-hose instability is usually associated with long-pulse LIAs, it is also problematic for high-current multi-pulse LIAs, because ion recombination and channel expansion times are so very long at typical residual gas pressures. For example, consider the Scorpius electron linear induction accelerator (LIA) being developed for multi-pulse flash radiography of large hydrodynamic experiments driven by high explosives [4]. Scorpius is designed to produce four 90-ns, 2-kA, 20-MeV pulses that will be focused onto a thin high-Z target to produce the radiographic source spots. Acceleration and transport of a 2-MeV injected beam by the 72 cells of the Scorpius LIA is illustrated in Figure 1. The inter-pulse delay time on Scorpius varies from ~100 ns to ~900 ns. Even for the longest inter-pulse delay, neither recombination nor channel ex-

pansion are fast enough to significantly affect the ion density. Therefore, the ion channel is expected to persist and its density to increase during the duration of the four-pulse burst from Scorpius. This would result in the same growth as a pulse four times the duration of a single Scorpius pulse [4].

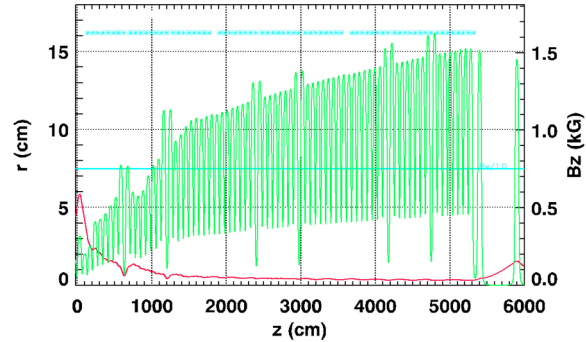


Figure 1: Solenoidal focusing of a 2-kA beam as it is accelerated from 2 MeV to 20 MeV by the Scorpius LIA. Green Curve: Solenoidal magnetic field on axis. Red Curve: Beam envelope radius. Cyan Asterisks: Axial location of 250-kV accelerating gaps. Cyan Line: Beam tube wall radius.

THEORY AND SIMULATIONS

The equations of motion for the beam centroid have been solved for the simple case of a beam interacting with a pre-formed channel in a uniform magnetic field [1, 2] using the spread-mass theory of [5] for Gaussian beam and channel profiles. The solution gives the fastest growing frequency $\omega_{i0} = 1.22(m_e \nu / m_i)^{1/2} c / R_{rms}$, where the factor of 1.22 comes from the detailed theory [2]. Here, R_{rms} is the rms beam radius, m_e and m_i are the electron and ion masses, and c is the speed of light. Also, $\nu = I / I_0$, with $I_0 = m_e c^3 / e = 17.045$ kA, and e is the electronic charge. Typical beam parameters and residual gases result in very low frequencies (< 30 MHz) [3], only two or three cycles during a beam pulse.

The analytic theory predicts that the maximum growth during a pulse is given by $\max(\xi / \xi_0) = \exp \Gamma(z)$ in the so-called linear regime, where ξ is the centroid position. The number of e-foldings of instability growth is $\Gamma(z) = 14.9 en_i z / B$, where B is the magnetic field. This

* Work supported by the U.S. Department of Energy and the National Nuclear Security Agency under contract DE-AC52-06NA25396.

† email address: cekdahl@lanl.gov

clearly shows that the fundamental driving force is proportional to the ion-channel electric field. Moreover, it shows that attenuation is due to the magnetic field, which also suppresses the beam-breakup (BBU) instability [6, 7].

After a beam pulse, the channel ion density decays as a result of recombination and channel expansion. We calculated the ion-density decay for durations much longer than the Scorpius inter-pulse delay time. Neither recombination nor channel expansion is fast enough to significantly affect the ion density in the time between two Scorpius pulses. Therefore, the ion density, and hose growth rate, will continue to increase for the entire four-pulse burst.

In order to determine the Scorpius vacuum requirements we simulated ion hose with the LAMDA beam dynamics code. (LAMDA is an acronym standing for Linear Accelerator Model for DARHT.) In LAMDA, the beam is modelled as a chain of non-interacting rigid disks. Parameters associated with each disk are the normalized current, energy, transverse centroid displacements, and radius. Each of these five quantities is a function of axial position, z , and the time measured back from the head of the pulse. Lorentz forces due to external magnetic fields, gaps, and conducting wall images are applied to each disk. The ion-hose algorithm in LAMDA adds a restoring force proportional to the separation of the beam and channel centroids, with parameters taken from analytic theory. This algorithm produces results in good agreement with the analytic theory, with particle-in-cell (PIC) simulations [8], and with experimental data [3].

We used the tune shown in Fig. 1 for these simulations, but we used a constant beam radius, as we did for earlier simulations of DARHT-II [2, 8]. Ionization of residual gas by a relativistic electron beam can be described by a neutralization fraction $f_e = n_i / n_e$, where n_e and n_i are the beam and ion densities. For typical LIA vacuum beam impact ionization proceeds according to $f_e = p_0 t / \alpha$ [2], where p_0 is the residual gas pressure and $\alpha = 1.1 \text{ Torr}\cdot\text{ns}$ for water vapour, which is the main constituent [9]. Thus, the ion density at any time late in the pulse train is simply that due to the beam time for all preceding pulses. The time between pulses is irrelevant, because decay of ion density is insignificant during that time.

To illustrate the instability, consider a train of four pulses having 80-ns flat-top, 10-ns rise and fall, and 200-ns start-to-start spacing (see Figure 2). This figure also shows the calculated ion density due to electron impact ionization of residual H_2O at 1000 nTorr pressure. This situation is unstable in the magnetic field of the Scorpius tune, as shown in Figure 3, which displays the relative growth of an initial 71-micron perturbation that is a sudden offset of the beam centroid from the magnetic axis. The plot shows the maximum instability amplitude during each pulse as it grows through the LIA. The wavelength of the oscillations in Figure 3 and Figure 4 is the betatron wavelength, which would also appear on a mismatched beam envelope.

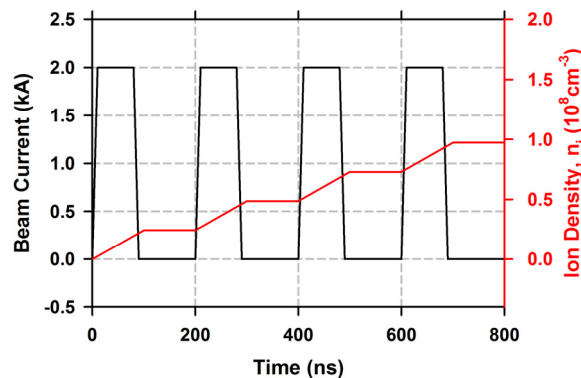


Figure 2: Pulse format used for simulations of ion-hose instability. Black Curve: Electron-beam current. Red Curve: Ion channel density from electron impact ionization of a $1.0\text{E-}6$ Torr residual pressure.

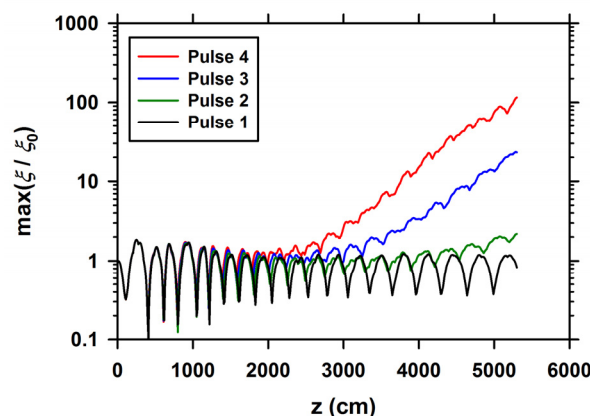


Figure 3: Growth of ion hose instability in $1\text{E-}6$ Torr on the four pulses shown in Figure 2. Black Curve: Pulse 1. Green Curve: Pulse 2. Blue Curve: Pulse 3. Red Curve: Pulse 4.

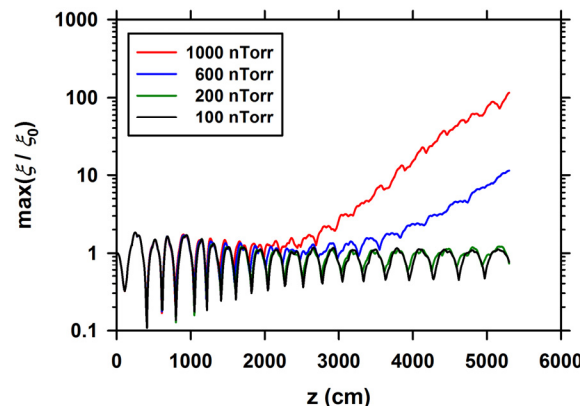


Figure 4: Ion hose instability growth on pulse 4 in Scorpius CDR tune for different residual pressures of H_2O . Red Curve: Residual pressure $1.0\text{E-}6$ Torr. Blue Curve: Residual pressure $6.0\text{E-}7$ Torr. Green Curve: Residual pressure $2.0\text{E-}7$ Torr. Black Curve: Residual pressure $1.0\text{E-}7$ Torr.

The nature of the motion at the exit of the accelerator is illustrated in Figure 5, which shows the trajectory taken by the beam centroid during pulse 4 for two pressures. The

beam rms radius at the accelerator exit is < 0.5 cm, so the motion for 600 nTorr would cause a significant enlargement of the focal spot due to motion blur. However, the motion for 200 nTorr would be acceptable. Therefore, ensuring that the Scorpius vacuum is less than 200 nTorr will prevent radiographic source-spot enlargement due to ion-hose motion. On DARHT-II this is accomplished by interlocking so that the accelerator cannot be operated if the vacuum is above 100 nTorr [3]. Based on these simulation results (Figure 4), we plan to use the same strategy on Scorpius.

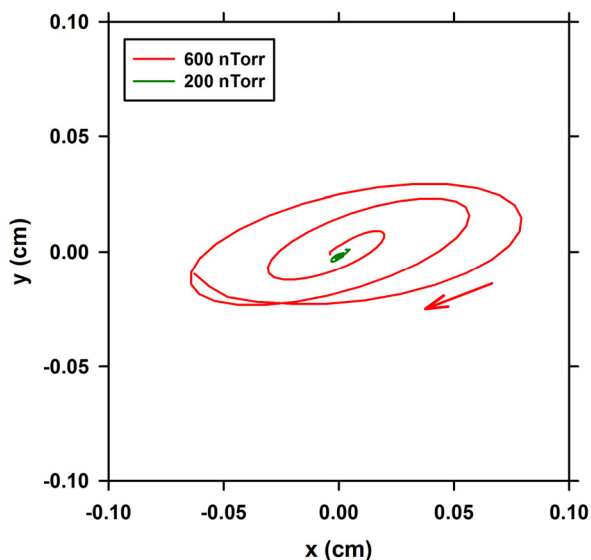


Figure 5: Trajectory of beam centroid during pulse 4 at the exit of the LIA. Red Curve: Residual pressure 600 nTorr. Green Curve: Residual pressure 200 nTorr.

Another source of ion-hose excitation might be beam injection with an offset from a preformed channel. Therefore, we also simulated growth excited with an offset starting at the beginning of the current flattop. The resulting ion hose growth is about a factor of four less for offset excitation than for excitation at the resonant frequency. However, resonant excitation, which is the worst case, is used as guidance for the Scorpius vacuum design.

CONCLUSION

Extensive simulations of the ion-hose instability have shown that a vacuum residual pressure of order 200 nTorr is required for the magnetic field to suppress it in the Scorpius LIA with the conceptual design tune. Thus, interlocking the Scorpius vacuum system at 100 nTorr should provide an adequate margin of safety for the ion-hose instability.

ACKNOWLEDGMENT

The author thanks his colleagues for invigorating discussions on this and other topics related to intense relativistic electron beams. He acknowledges interesting discussions with Y.-J. Chen, J. Ellsworth and N. Pogue from LLNL. Special thanks go to C. Thoma of Voss Scientific for his expert support of the LAMDA code. Finally, the author is indebted to B. Trent McCuistian for a thorough review of this article.

REFERENCES

- [1] H. L. Buchanan, "Electron beam propagation in the ion-focused regime," *Phys. Fluids*, vol. 30, pp. 221 - 231, 1987.
- [2] T. C. Genoni and T. P. Hughes, "Ion-hose instability in a long-pulse linear induction accelerator," *Phys. Rev. - ST Accel. Beams*, vol. 6, no. 4, p. 030401, 2003.
- [3] C. A. Ekdahl, E. O. Abayta, P. Aragon and et al., "Long-pulse beam stability experiments on the DARHT-II linear induction accelerator," *IEEE Trans. Plasma Sci.*, vol. 34, pp. 460-466, 2006.
- [4] C. Ekdahl, "Beam dynamics for the Scorpius Conceptual Design Report," Los Alamos National Laboratory Report LA-UR-17-29176 and arXiv:1710.11610, 2017.
- [5] E. P. Lee, "Resistive hose instability of a beam with the Bennett profile," *Phys. Fluids*, vol. 21, no. 8, p. 1327, 1978.
- [6] C. Ekdahl, E. O. Abeyta, R. Archuleta, H. Bender, W. Broste, C. Carlson, G. Cook, D. Frayer, J. Harrison, T. Hughes, J. Johnson, E. Jacquez, B. T. McCuistian, N. Montoya, S. Nath, K. Nielsen, C. Rose, M. Schulze, H. V. Smith, C. Thoma and C. Y. Tom, "Suppressing beam motion in a long-pulse linear induction accelerator," *Phys. Rev. ST Accel. Beams*, vol. 14, no. 12, p. 120401, 2011.
- [7] J. E. Coleman, D. C. Moir, C. A. Ekdahl, J. B. Johnson, B. T. McCuistian, G. W. Sullivan and M. T. Crawford, "Increasing the intensity of an induction accelerator and reduction of the beam breakup instability," *Phys. Rev. STAB*, vol. 17, no. 3, p. 030101, 2014.
- [8] Y. Tang, T. P. Hughes, C. Ekdahl and M. E. Schulze, "Implementation of spread mass model of ion hose instability in LAMDA," in *Part. Accel. Conf.*, Albuquerque, NM, USA, 2007.
- [9] H. A. Davis, R. T. Olson and D. C. Moir, "Neutral desorption from intense electron beam impact on solid surfaces," *Phys. Plasmas*, vol. 10, no. 8, pp. 3351 -3357, 2003.